JOURNAL OF Applied Polymer SCIENCE

Effect of Boron Nitride as a Nucleating Agent on the Crystallization of Bacterial Poly(3-hydroxybutyrate)

Jorge Arturo Soto Puente,[1,2] Antonella Esposito,[1] Frédéric Chivrac,[2] Eric Dargent[1]

[1]AMME-LECAP EA4528 International Laboratory, Institut des Matériaux de Rouen, Université de Rouen, BP12 Saint Etienne du Rouvray Cedex 76801, France

[2]CREAGIF Biopolymères, 18 avenue de la voie aux coqs, Bretteville sur Odon 14760, France

Correspondence to: E. Dargent (E-mail: eric.dargent@univ-rouen.fr)

ABSTRACT: Different concentrations of boron nitride (BN) (0.2–0.8 wt %) are added to poly (3-hydroxybutyrate) (PHB) as a nucleating agent. Polarized Optical Microscopy (POM) coupled to Differential Scanning Calorimetry (DSC) allow to monitor the isothermal and nonisothermal crystallization of neat and nucleated PHBs. It is found that the addition of BN to PHB modifies the mechanisms of crystallization without changing the crystallinity degree. DSC can replace POM whenever POM does not allow to estimate the spherulites growth rate. The Hoffman-Lauritzen theory is used to explain the role of BN. The nucleating agent allows polymer crystallization at lower supercooling degrees. The regime II of crystallization is observed for nucleated PHBs. A modification of the coupling effect between the amorphous and the crystalline phases is evidenced. It is shown that a concentration of 0.2 wt % BN is sufficient to decrease the glass transition temperature and modify the crystallization mechanisms of PHB. © 2012 Wiley Periodicals, Inc. J. Appl. Polym. Sci. 000: 000–000, 2012

KEYWORDS: crystallization; particle nucleation; biopolymers; differential scanning calorimetry (DSC)

Received 18 May 2012; accepted 11 June 2012; published online
DOI: 10.1002/app.38182

INTRODUCTION

Polyhydroxyalkanoates (PHAs) are bio-sourced linear polyesters spontaneously produced by some bacteria via the fermentation of sugars or lipids to store energy in conditions of physiological stress.[1] Thanks to their biodegradability, biocompatibility, and tunable mechanical properties, PHAs have been quickly identified as good candidates to replace fossil-based commodity polymers.[2] Nevertheless, their industrial development and the corresponding commercial applications are not comparable yet to those of other biopolymers such as poly (lactic acid) (PLA), for which processing and mechanical properties are well known and controlled, and whose commercial applications in food packaging are already proficient.[3] The most common bacterial PHAs is poly (3-hydroxybutyrate), also referred as PHB or P3HB. Besides classical bacterial fermentation processes (with e.g., *Ralstonia Eutropha)*, new biosynthesis pathways have been developed since 2009, such as transgenic plants (e.g., *Panicum virgatum*).[4] Nevertheless, whatever its source, PHB suffers from several deficiencies which considerably limit its applications. One may mention its extreme brittleness due to its high crystallinity and a narrow processing window, induced by a melting temperature which is close to its degradation temperature.[5] Moreover, during crystallization PHB develops very large spherulites as a consequence of an extremely low nucleation density.[6] In addition, the glass transition temperature of the residual amorphous phase is low enough to let the polymer chains keep on reorganizing even after cooling down to room temperature, i.e., PHB crystalline fraction tends to increase with time and the polymer grows brittler. So far, many strategies to overcome brittleness and to enhance the crystallization rate of PHB have been studied. These strategies include either blending PHB with other polymers such as poly (vinyl acetate-*co*-vinyl alcohol),[7] or copolymerizing the hydroxybutyrate (HB) monomers with hydroxyvalerate (HV) monomers (PHBV),[8] or with hydroxyhexanoate (HHx) monomers (PHBHHx).[9] Whatever the explored strategy, the crystallization rate usually remains slow enough to cause serious problems during processing. For instance, the polymer tends to be sticky during extrusion and stays soft once molded, even after long cooling times, making it difficult to eject. The crystallization mechanisms can be modified by adding a nucleating agent to the polymer, so that the grown spherulites will be smaller and more homogenous in size.[6] Many nucleating agents have been studied so far, including thymine and melamine,[6] boron nitride, talc, zinc stearate, hydroxyapatite,[5] terbium oxide, lanthanum oxide,[10] cyclodextrin-complex.[11] Liu et al.[10] showed that the best nucleating effect on PHBV

© 2012 Wiley Periodicals, Inc.

crystallization is observed when BN is used; Wang et al.[5] found that the best nucleating effect on P(3HB-*co*-4HB) crystallization is obtained when the concentration of BN is 0.5 wt %. In this study, the crystallization behaviors of neat and nucleated PHB are compared for different BN concentrations. Many works dealing with the crystallization behavior of polymers described by the Avrami or Ozawa analyses are available in the literature[12,13] but only few of them used the Hoffman-Lauritzen model[14] to get some more information about the role of the nucleating agent. The mechanism by which crystals grow on the nucleating particles is still a source of debate.[15] It has been proposed that crystal nuclei pack densely along the particle surface, thus limiting lamellar thickness.[16–18] In addition, it has been observed that the growth rate of the spherulites is generally not affected by the addition of fillers; however, the presence of a nucleating agent typically leads to finer crystalline microstructures without any significant change in the maximum crystallinity degree.[15] In this work, the thermodynamic parameters and the nucleation behavior of neat and nucleated PHBs were studied by means of the Avrami and Hoffman-Lauritzen models in order to better explain the role of the boron nitride on polymer crystallization.

EXPERIMENTAL

Materials and Samples Preparation

PHB was supplied by Biomer, Germany. The weight-average molecular weight before extrusion was 4×10^5 g mol^{-1}. Boron Nitride (BN) grade NX1 is a mineral powder used as a nucleating agent and was purchased from Momentive Perfomance Materials, France. The powder has a hexagonal graphitic crystalline lattice and a mean particle size of 5 μm. Samples were processed by a DSM Xplore twin-screw micro-compounder. The extrusion temperature was set at 185°C and the screw rotation speed was 100 rpm. BN NX1 was added to PHB at different concentrations, between 0.2 and 0.8 wt %. Neat PHB and its compounds were then injected. The temperature of the mold was set at 60°C.

Characterization Techniques

Differential Scanning Calorimetry (DSC) was performed by a Perkin Elmer 8500 equipment to monitor the crystallization and melting processes of neat and nucleated PHBs. Energy and temperature calibration were performed with indium and zinc standards. The glass transition temperature (T_g) was measured by a TA 2920 calorimeter whose calibration was performed with an indium standard. All the measurements were performed under nitrogen to prevent oxidative degradation. For each experiment a fresh sample was used (about 10 mg). The samples were analyzed by two thermal programs:

Program I. Classical Scan. Samples were heated to 190°C at a heating rate of 10°C min^{-1} and annealed for 1 min to melt all the crystals previously formed. Then, they were cooled at 10°C min^{-1} to −30°C and finally heated again to 190°C. To determine T_g the samples were quenched from the melt to get the polymer in its glassy state with as much amorphous phase as possible and then heated to 30°C at a rate of 10°C min^{-1}.

Program II. Isothermal Crystallization. Samples were heated to 190°C at a rate of 80°C min^{-1} and annealed for 1 min. Then they were quenched as fast as possible to the crystallization temperature (T_c) and kept in isothermal conditions until crystallization is achieved.

Polarized Optical Microscopy (POM) observations were performed on a Nikon microscope equipped with a Sony CCD-IRIS camera. Each sample was placed between two glass slides, then heated onto a Mettler FP82 HT hot stage to 190°C at 10°C min^{-1} and annealed for 1 min. Finally, the samples were quickly placed on a second hot stage previously set at the defined crystallization temperature (T_c). Pictures were taken every 30 s and analyzed by the software ImageJ.

Wide Angle X-ray Diffraction (WAXD) was performed on a D8 Advance BRUKER AXS machine equipped with a CoK_α radiation source ($\lambda = 0.179$ nm). X-ray spectra were obtained for angles between 10° and 40° at 35 kV and 40 mA. The scanning speed was set at 0.1 s/step and the angle increment was 0.04° s^{-1}. The calculation of the crystallinity degree X_c was carried out by dividing the area under the crystalline peaks by the total area (crystalline peaks plus the amorphous scattering contribution).

RESULTS AND DISCUSSION

Before studying the influence of BN NX1 on PHB crystallization, a thermal characterization of neat PHB was accomplished. *Program I* was used to investigate its crystallization and melting behavior (Figure 1). During cooling, a crystallization peak was recorded between 110 and 70°C. During heating, the heat flow step associated to the glass transition was observed between −5 and 10°C and the melting profile included two endothermic peaks starting at 140°C. According to the literature, the lower melting temperature ($T_{m1} = 166$°C) is to be attributed to the crystals created during the cooling step of *Program I*, whereas the higher melting temperature ($T_{m2} = 173$°C) should rather be attributed to the crystals formed by recrystallization (or crystal rearrangement) during the heat scan of the thermal program.[6,10,19]

The spherulitic growth of neat PHB could be monitored by POM during cooling or under isothermal conditions (see the example in Figure 2). The crystallization temperature range used for POM monitoring was defined on the basis of the crystallization temperature range previously observed by DSC (Figure 1). The average diameter of the spherulites appeared quite large (close to 800 μm, see Figure 2) and the image sequences were used to estimate the isothermal spherulitic growth rate (G), which turned out to be relatively low. By reiterating this method in isothermal conditions at different crystallization temperatures, an average value of G for several crystallization temperatures could be obtained. Figure 3 shows the dependence of the average radial growth rate on the crystallization temperature, as it is typically obtained for many polymers.[20] As for neat PHB, the maximum value for G is observed for a crystallization temperature close to 93°C; this result is in good agreement with the values reported in the literature.[21]

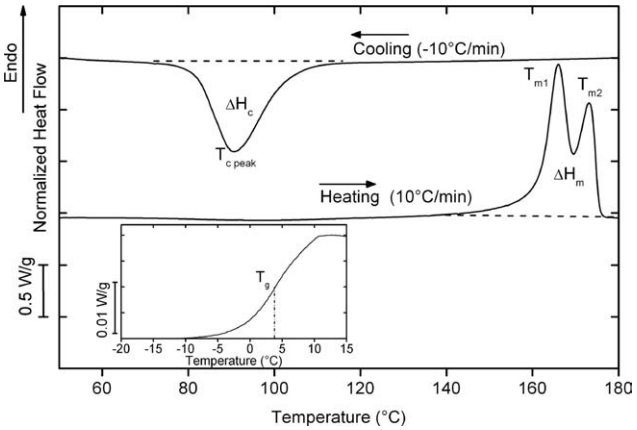

Figure 1. DSC curves of neat PHB obtained by *Program I*.

The Hoffman-Lauritzen theory[22] (H-L theory) was also used to study the crystallization of neat PHB. The H-L theory states that the crystallization process can be described by three different growth regimes depending on the degree of supercooling, i.e., $T_m - T_c$. In particular, the growth is supposed to progress through successive nucleation steps occurring on the surfaces of the growing crystals.[20] Regime I is typically observed when the crystallization temperature T_c is close to the melting temperature T_m. In this case, the growth rate G is proportional to the surface nucleation rate i, and the substrate completion rate g is higher than i. This means that any n layer of folded polymer chains will be completed before the next $n+1$ layer is initiated. As the crystallization temperature T_c starts to decrease with respect to the melting temperature T_m, a transition is observed from Regime I to Regime II. In Regime II, G is proportional to $i^{1/2}$ and the rates g and i become comparable as a consequence of the rapid increase of the surface nucleation rate, itself associated to a higher degree of supercooling ($T_m - T_c$).[23] Therefore, several acts of nucleation take place at the same time and on the same crystalline surface; the consequence is that the crystal growth proceeds even if a given layer of folded polymer chains is not yet completely filled. As the crystallization temperature T_c gets even lower with respect to the melting temperature T_m, another transition is observed from Regime II to Regime III. In Regime III, the growth rate G is controlled by i rather than by $i^{1/2}$. This means that there is a profusion of very small nuclei and, therefore, the rate g is much lower or eventually nil. The growth front, then, is extremely rough and irregular because of such an intensive and multiple nucleation process. The H-L equation[22] describes the radial growth rate of the spherulites as following

$$G = G_0 e^{\left(-U^*/R(T_c - T_\infty)\right)} e^{\left(-K_g/f\,T_c \Delta T\right)} \quad (1)$$

where G_0 is an independent temperature constant, U^*=17 250 J mol^{-1} is the activation energy for the transport phenomena of the crystallizable polymer segments (the polymer chains have to be transported through the melt onto the surface of the growing crystal),[24] R = 8.31 J mol^{-1} K^{-1} is the gas constant, T_c is the crystallization temperature, T_∞ is the temperature at which all the molecular motions related to the viscous flow stop, defined as $T_\infty = T_g - C$ where C = 51.6°C is a constant from the Williams-Landel-Ferry law,[25] ΔT is the supercooling degree, given by $\Delta T = T_m^0 - T_c$ where T_m^0 is the equilibrium melting temperature of the polymer (i.e., the theoretical melting temperature of the polymer supposed to be 100% crystalline), K_g is the nucleation constant[26] and f is defined as[22]

$$f = 2T_c/(T_m^0 + T_c) \quad (2)$$

Program II was used to apply the Hoffman-Weeks method (H-W method)[27] in order to determine T_m^0 for neat PHB. Every PHB sample, originally crystallized in isothermal conditions at a given crystallization temperature T_c was heated again to the melting temperature at a rate of 10°C min^{-1}. The H-W method requires plotting the T_m values (measured during heating) vs. the T_c values (set during isothermal crystallization). These experimental points are expected to align if the lamellar thickness is proportional to the degree of supercooling.[28]

The value of T_m^0 is then obtained by extrapolating this straight line to $T_m = T_c$ (not shown here).[29,30] Neat PHB showed two endothermic peaks between 165 and 175°C (Figure 1).

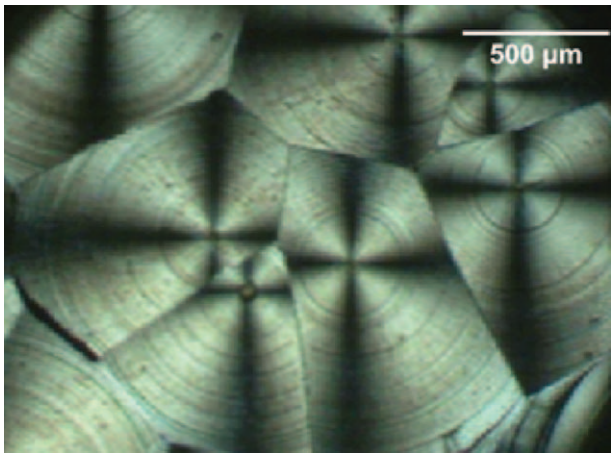

Figure 2. POM image of neat PHB crystallized at T_c = 95°C.

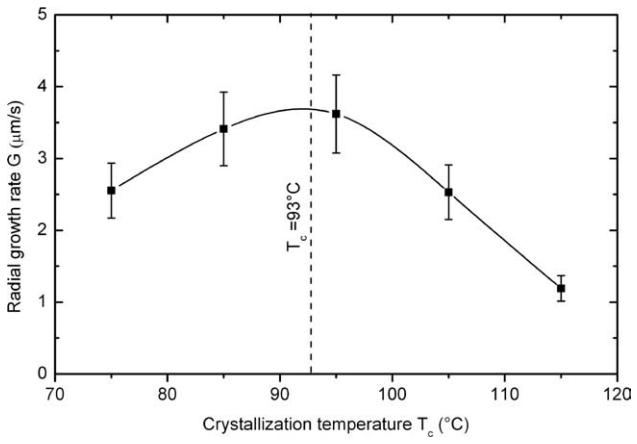

Figure 3. Radial growth rate of spherulites (G) of neat PHB as a function of the crystallization temperature (T_c).

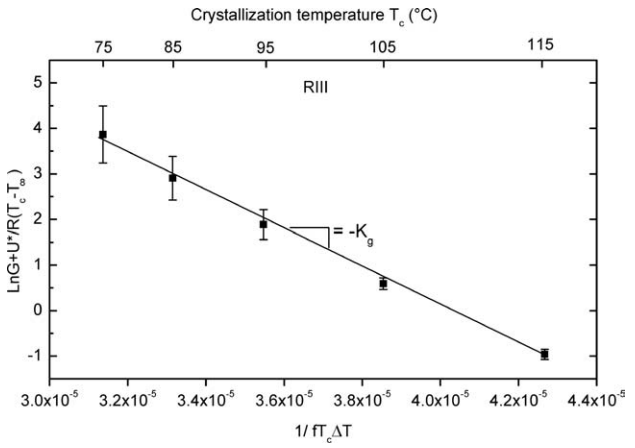

Figure 4. Linearized H-L equation for neat PHB (G obtained with POM experimental conditions).

However, the crystallization temperature T_c affected only the first endothermic peak, whereas it had a negligible effect on the second one. Therefore, the H-W method for neat PHB was performed by taking into account only the lower melting temperature T_{m1}. The value obtained with this method was $T_m^0 = 180.5 \pm 4.5$°C.

By linearizing and rearranging the H-L equation [eq. (1)], the following equation is obtained

$$\ln G + {}^{U^*}/_{R(T_c - T_\infty)} = \ln G_0 - {}^{K_g}/_{f\,T_c \Delta T} \qquad (3)$$

By plotting $\ln G + U^*/R(T_c - T_\infty)$ as a function of $1/fT_c\Delta T$, the nucleation constant (i.e., the slope of the straight line, $-K_g$) and the independent temperature constant (i.e., the intercept of the straight line, $\ln G_0$) were calculated. Figure 4 shows the values obtained for neat PHB at different values of T_c. The T_g value for neat PHB is reported in Table I. Once again, the value of T_∞ was determined by using the T_g values obtained by *Program I*. Figure 4 shows a single slope straight line which means that the growth regime is the same on the overall crystallization temperature range (75–115°C). A transition between Regime III and Regime II for neat PHB and its copolymers has been previously reported in the literature between 120 and 140°C.[31] In this work, the temperatures set for the isothermal crystallization of neat PHB were lower than 120°C; therefore, only crystallization in the Regime III could be observed. A value of 4.2×10^5 K^2 was obtained for the nucleation constant K_g. This value is in good agreement with the value of 3.1×10^5 K^2 reported in the literature by Peng et al.[26] for crystallization of PHBV (8 mol % HV) at temperatures comprised between 70 and 120°C. After neat PHB, nucleated PHB samples were characterized. First of all, WAXD analysis was performed to check the possible influence of the nucleating agent on the crystalline structure of the polymer matrix. Figure 5 shows WAXD patterns for neat and nucleated PHBs. All the samples, both neat and nucleated ones, showed the same characteristic diffraction peaks. The peaks observed at 15.7°, 19.8°, and 25° are characteristics of the (020), (110) and (101) crystallographic planes of PHB unit cell respectively.[32,33] The diffraction peak at 31.2° is entirely due to the presence of BN crystals[34] and, as expected, its magnitude increased along with the BN NX1 concentration. This means that the orthorhombic structure of PHB crystals was not modified by the presence of the nucleating agent. The crystallinity degree of all the samples could also be obtained from the WAXD patterns (Table I). Whatever the method used, the X_c values reported in Table I shows that the presence of the nucleating agent does not significantly affect the crystallinity degree of the sample, whatever the concentration of BN NX1. *Program I* was then applied to the nucleated PHB samples, as shown in Figure 6. The crystallization from the melt of nucleated PHBs occurred at higher temperatures with respect to what observed for neat PHB (~ 30°C higher) and this phenomenon is observed even for low concentrations of the nucleating agent. As expected, the particle surfaces of the nucleating agent acted as crystalline substrates onto which the polymer chains were more easily adsorbed and folded. Figure 1 shows that the melting process of neat PHB is represented by a double endothermic peak; nucleated PHBs, on the other hand, showed a single modal melting behavior ($T_m \approx 170$°C) (Figure 6). The T_m^0 values calculated with the H-W method are reported in Table I with the corresponding standard deviation. The value of the equilibrium melting temperature seems to slightly increase with an increasing content of nucleating agent; however, standard deviation values show that the differences are not significant. The crystallinity degree X_c was calculated from the DSC curves as

$$Xc = {}^{\Delta H_m}/_{\Delta H_m^0} \qquad (4)$$

where $\Delta H_m^0 = 146$ J g^{-1} is the equilibrium melting enthalpy (i.e., the theoretical melting enthalpy of the polymer supposed to be 100% crystalline)[10] and ΔH_m is the melting enthalpy calculated from the endothermic peak recorded during the second heating step in *Program I*. Table I reports the X_c values obtained from DSC scans [eq. (4)] in comparison with the values obtained from WAXD patterns. The two techniques gave similar X_c values. As previously observed by Sobkowicz et al.,[15] the presence of BN NX1 particles had a significant effect on the

Table I. Glass Transition and Crystallization Temperatures Obtained by DSC, Width of the Glass Transition $\Delta T_{16\text{–}84\%}$, Crystallinity Degrees and T_m^0 Values Obtained by H-W Method for Neat and Nucleated PHB

Sample	T_g (°C)	$\Delta T_{16\text{-}84\%}$ (°C)	Peak T_c (°C)	X_c (DSC) (%)	X_c (WAXD) (%)	T_m^0 (°C)
PHB	4 ± 0.5	10.1 ± 1	91 ± 0.5	60 ± 5	55 ± 5	180.5 ± 4.5
+BN NX1 0.2 %	1 ± 0.5	8.6 ± 1	121 ± 0.5	63 ± 5	61 ± 5	182.0 ± 5.0
+BN NX1 0.4 %	1 ± 0.5	8.9 ± 1	122 ± 0.5	63 ± 5	59 ± 5	183.0 ± 5.0
+BN NX1 0.8 %	1 ± 0.5	9.4 ± 1	125 ± 0.5	65 ± 5	58 ± 5	185.0 ± 5.0

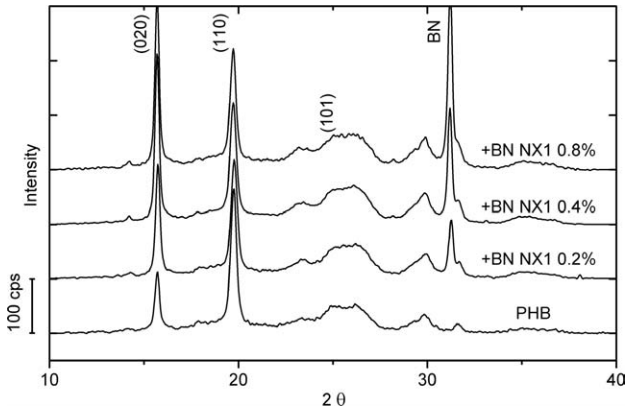

Figure 5. WAXD pattern of neat and nucleated PHB.

crystallization temperature range but almost no effect on the maximum crystallinity degree, no matter their concentration. A slight effect on the glass transition temperature T_g was also observed, but only when neat PHB is compared to nucleated PHBs. In polymers, glass transition occurs over a large temperature interval (ΔT_g) and is associated to a variation of the specific heat capacity at constant pressure (ΔC_p). According to Donth's method,[35] the temperature interval $\Delta T_{16-84\%}$, which is comprised between $\Delta C_p = 16\%$ and $\Delta C_p = 84\%$, informs about the amorphous phase mobility and the distribution of the relaxation times at T_g.[36,37] When the nucleating agent was added to the polymer, the decrease of the T_g value was accompanied by a slight tendency of the $\Delta T_{16-84\%}$ value to decrease, as well. Even if the corresponding standard deviation does not make the $\Delta T_{16-84\%}$ decrease extremely significant, such evidence, associated to the clear tendency about T_g, would mean that the presence of the nucleating agent slightly decreased the rigidity of the amorphous phase, made its mobility more cooperative and reduced the width of the distribution of relaxation times at T_g.[38] The most probable explanation is that, as the crystalline and the amorphous phases in semicrystalline polymers are generally not independent from each other,[39] any change in the crystallinity degree and/or in the microstructure of the crystalline phase can lead to a modification of the chain mobility in the amorphous phase.[40,41] $\Delta T_{16-84\%}$ and T_g values would suggest that the amorphous and the crystalline phases are less coupled in nucleated PHBs than in neat PHB. Such a difference in the morphology of the crystalline phase was readily detected by POM. In fact, nucleated PHBs developed a morphology which was definitely too fine to be observed by POM, whereas the spherulitic growth of neat PHB could be easily monitored during cooling or under isothermal conditions, as previously stated (Figure 2). As the spherulites of nucleated PHBs were too little to be measured, their average diameter was estimated to be inferior to the microscope resolution, i.e. less than 10 μm (vs. 800 μm for neat PHB). The size of PHB spherulites dramatically changed upon addition of a nucleating agent, which prevented from calculating a value of spherulitic growth rate (G) on the basis of direct POM observations. As a consequence, a better insight in the effects of BN NX1 on PHB crystallization kinetics was obtained by using a model derived from the H-L equation [eq. (1)]. Indeed, it is possible to investigate the crystallization behavior of a polymer by exploiting DSC data obtained under isothermal conditions (*Program II*).[19] The linear growth rate of the spherulites (G) can be then expressed as a function of two parameters, Z and n, by using the Avrami model

$$G \propto Z^{1/n} \tag{5}$$

where n is the Avrami exponent, related to the mechanism of nucleation as well as to the dimensionality of crystal growth, and Z is a time parameter, depending on the crystallization temperature T_c and containing both nucleation and growth contributions.[42,43] To obtain n and Z values, the *Program II* and then the Avrami equation were applied

$$1 - X(t) = \exp(-Zt^n) \tag{6}$$

where $X(t)$ represents the fraction of crystallized material as a function of the crystallization time t, scaled by the induction time under isothermal conditions at T_c.[44] By linearizing and plotting eq. (6) (graph not shown), the slope (n) and the intercept (log Z) were obtained. These values are resumed in Table II. According to the typical values of the Avrami parameters reported in the literature,[12,45] n values between 2 and 3 suggest, in conditions of sporadic nucleation, a two-dimensional crystal growth for neat PHB. On the other hand, higher n values (between 3 and 4) would indicate, in whatever condition of nucleation, a three-dimensional crystal growth for nucleated PHBs. At any given crystallization temperature T_c the n parameter appeared slightly increased by the increased concentration of nucleating agent. Table II resumes also the values obtained for the Z parameter and, more rigorously, the values derived for the $Z^{1/n}$ parameter (whose measurement unit does not depend on n), as previously pointed out by Maffezzoli et al.[44] The values of Z and $Z^{1/n}$ reported in Table II are temperature dependent and increase with the decrease of the crystallization temperature. This is reasonable because Z and $Z^{1/n}$ are related to the crystallization rate, which increases with the supercooling degree.

By combining eqs. (1) and (5), the crystallization kinetics could be finally expressed as

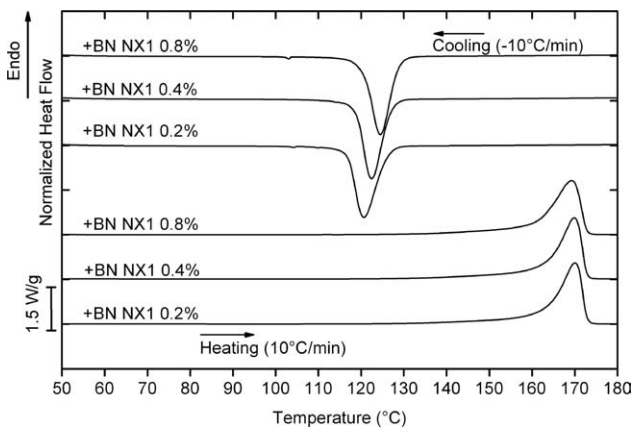

Figure 6. DSC thermograms showing the crystallization and the melting of nucleated PHB.

Table II. Avrami Parameters for Neat and Nucleated PHB at Different Crystallization Temperatures

Sample	T_c (°C)	100	105	110	115	120	125
PHB	n	2.6	2.6	2.6	2.4	2.4	2.6
	$Z(1/s^n)$	1.2×10^{-5}	1.6×10^{-6}	4.7×10^{-7}	5.5×10^{-7}	5.4×10^{-8}	3.2×10^{-9}
	$Z^{1/n}(1/s)$	$1^{-}.2 \times 10^{-2}$	5.6×10^{-3}	4.0×10^{-3}	2.5×10^{-3}	9.9×10^{-4}	5.6×10^{-4}
	T_c (°C)	125	130	135	140	145	150
+BN NX1 0.2 %	n	2.8	2.8	3.0	2.9	2.9	-
	$Z(1/s^n)$	1.5×10^{-5}	1.7×10^{-6}	3.8×10^{-8}	6.6×10^{-9}	9.1×10^{-10}	-
	$Z^{1/n}(1/s)$	1.8×10^{-2}	8.0×10^{-3}	3.2×10^{-3}	1.4×10^{-3}	6.9×10^{-4}	-
+BN NX1 0.4 %	n	-	2.8	3.2	2.9	2.9	3.0
	$Z(1/s^n)$	-	2.8×10^{-6}	4.3×10^{-8}	2.2×10^{-8}	3.0×10^{-9}	1.0×10^{-10}
	$Z^{1/n}(1/s)$	-	1.1×10^{-2}	4.7×10^{-3}	2.1×10^{-3}	1.0×10^{-3}	5.3×10^{-4}
+BN NX1 0.8 %	n	-	3.1	3.2	3.4	3.0	3.8
	$Z(1/s^n)$	-	2.7×10^{-6}	9.8×10^{-8}	1.9×10^{-9}	3.3×10^{-9}	1.1×10^{-12}
	$Z^{1/n}(1/s)$	-	1.5×10^{-2}	6.3×10^{-3}	2.8×10^{-3}	1.6×10^{-3}	7.3×10^{-4}

$$\ln Z/n + U^*/R(T_c - T_\infty) = \ln G_0 - K_g/f\,T_c\Delta T + C \qquad (7)$$

where C is an adjustable constant. Therefore, the nucleation constant K_g could also be obtained, similarly to the procedure shown about eq. (3), by plotting $\ln Z/n + U^*/R(T_c - T_\infty)$ as a function of $1/fT_c\Delta T$, where the n and Z parameters were obtained by the Avrami model (*Program II*). Once more, a straight line was obtained whose slope is given, apart from the negative sign, by K_g. Figure 7 shows two set of data for neat PHB, one plotted from eq. (3) (standard H-L model) and the other from eq. (7) (rearranged H-L equation). The two set of data are parallel; they follow the same linear variation but are shifted on the $\ln Z/n + U^*/R(T_c - T_\infty)$ axis. The reason is that the rearranged and the standard H-L equations differ in a term (the proportionality constant C suggested by eq. (5)) that fortunately does not affect the nucleation constant K_g (i.e., the slope of the straight line). Both the straight lines obtained with the two methods (POM and eq. (3) vs. DSC and eq. (7)) have the same slope (± 0.1%); therefore, these two methods are in good agreement with each other and both of them can be used to calculate the nucleation constant K_g. For the nucleated PHBs, the values are shifted to higher temperatures and seem independent on the BN content. A slope change was observed when the crystallization temperature T_c ranged from 135 to 140°C. The nucleation constant K_g depends on several parameters, including the lateral surface free energy (σ) and the fold surface free energy (σ_e) of the crystalline lamellae. This dependence is expressed as[22]

$$K_g = rb_0\sigma\sigma_e T_m^0 \Big/ k\Delta H_m^0 \qquad (8)$$

where r is a parameter related to the crystal growth regime as described by the Hoffman model ($r = 4$ for Regimes I and III, whereas $r = 2$ for Regime II),[46] $b_0 = 5.8 \times 10^{-10}$ m is the expected thickness of the folding polymer unit calculated from the average dimensions of PHB orthorhombic crystalline unit cell,[47] $k = 1.38 \times 10^{-23}$ J K^{-1} is the Boltzmann constant, T_m^0 and ΔH_m^0 are the equilibrium melting temperature and enthalpy respectively. Hoffman and Lauritzen[48] explained, in their pioneer work, that the lateral surface free energy (σ) could be supposed constant whatever the crystal growth regime. In fact, during crystallization, the lateral surfaces of the growing crystals are not connected to the surrounding supercooled melt polymer through covalent bonds and, as a consequence, σ depends only on the chemical composition and the crystallographic parameters of the crystalline growing phase. For this reason, σ could be calculated by the empirical equation proposed by Thomas-Stevely and reported by Lauritzen and Hoffman[49]

$$\sigma = \beta\Delta H_m^0 (a_0 b_0)^{1/2} \qquad (9)$$

where β is a dimensionless constant that depends on the polymer structure ($\beta \sim 0.25$ for polyesters),[50–52] ΔH_m^0 is the equilibrium melting enthalpy, $a_0 = 6.6 \times 10^{-10}$ m and b_0 are the width and the thickness of the folding polymer unit respectively.[47] By using these parameters, a value of $\sigma = 2.9 \times 10^{-2}$ J m^{-2} was obtained.

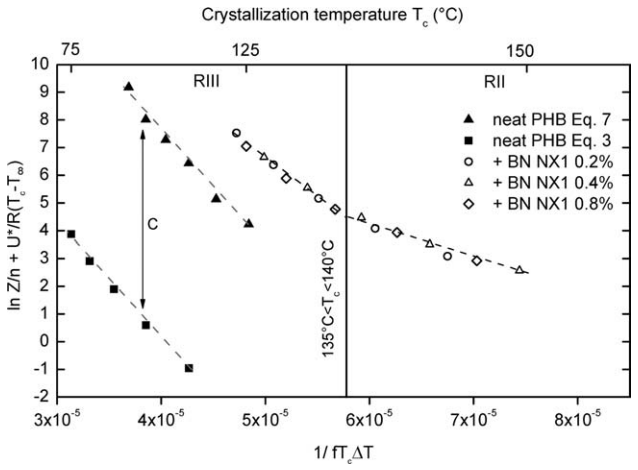

Figure 7. Crystallization kinetics according to the H-L model (from eq. (7)) for neat and nucleated PHB.

Table III. Nucleation Constants $K_{g(III)}$ and $K_{g(II)}$, the Ratio $K_{g(III)}/K_{g\ (II)}$ and the Fold Surface Free Energies for Neat and Nucleated PHB

Sample	$K_{g(III)}$ (K^2)	$K_{g(II)}$ (K^2)	$K_{g(III)}/K_{g\ (II)}$	$\sigma_{e(III)}$ (J/m^2)	$\sigma_{e(II)}$ (J/m^2)
PHB	4.2×10^5	-	-	3.6×10^{-2}	-
+BN NX1 0.2 %	3.0×10^5	1.4×10^5	2.1	2.5×10^{-2}	2.4×10^{-2}
+BN NX1 0.4 %	2.3×10^5	1.2×10^5	1.9	2.0×10^{-2}	2.1×10^{-2}
+BN NX1 0.8 %	2.6×10^5	1.3×10^5	2.0	2.2×10^{-2}	2.3×10^{-2}

Once the values of σ calculated by eq. (9) and the values of K_g obtained either by the standard or by the rearranged H-L equation (eq. (3) or eq. (7)), eq. (8) gave the corresponding values of the fold surface free energy (σ_e) of the crystalline lamellae for all the samples in any of their crystal growth regimes. The values of the nucleation constant (K_g) and the fold surface free energy (σ_e) for both the growth Regimes III and II are listed in Table III. According to eq. (8) and coherently with the definition of the r parameter, the $K_{g(III)}/K_{g(II)}$ ratio is equal to 2 whenever a transition from the growth Regime III to the growth Regime II occurs.[49] Looking at the crystallization kinetics obtained for the nucleated PHBs (Figure 7), a slope change was observed when the crystallization temperature T_c ranged from 135 to 140°C. This phenomenon, associated to the expected value for the $K_{g(III)}/K_{g(II)}$ ratio (Table III), confirmed the change in the growth regime announced in the literature for a crystallization temperature ranging from 120 to 140°C.[31] As previously stated, such a change could not be observed for neat PHB (Figure 4) because of a crystallization temperature range (75–115°C) lower than the expected temperature range (120–140°C) for Regime II to Regime III transition. Table III shows that, in the explored temperature range, σ_e does not depend on the crystal growth regime. Similar results were obtained for polypropylene crystallized in Regime II and III.[53] The fold surface free energy σ_e has a major influence on another energy parameter which is known as the work of chain folding (q), i.e., the energy required to the polymer to bend its chains back upon themselves when folding on a growing crystal lamellae. The dependence of the work of chain folding on σ_e is expressed as[48]

$$q = 2a_0 b_0 \sigma_e \tag{10}$$

where, once again, a_0 and b_0 are the width and the thickness of the folding polymer unit. By using eq. (11), the work of chain folding per mole of polymer could be estimated for both neat and nucleated PHBs (q = 16.6 kJ mol^{-1} for PHB vs. q = 10.4 kJ mol^{-1} for nucleated PHBs). Previous works reported that q is somehow linked to the stiffness of the polymer chains.[7,26,53] In this study, however, there is no difference in the chemistry of the macromolecules which could explain the decrease of σ_e and the subsequent decrease of q. Hoffman proved that the "variable cluster" model appropriately describes Regime III mechanisms.[23] In this model the adjacent chain folding occurs in small clusters. The clusters are connected together by chains with amorphous character. The intraspherulitic amorphous fraction is then partially due to the amorphous connections between any two adjacent or non-adjacent clusters of folding chains. This model suggests that in the case of neat PHB, the surfaces of the growing lamellae would contain regularly folded polymer chains but also a considerable fraction of tie macromolecules and/or polymer chains forming loops. On the other hand, the crystal growth of nucleated PHBs, which occurs at lower supercooling degrees, would contain less "mistakes" and progress more regularly.

Despite the limits of the Avrami model to describe the crystallization phenomena in details, its relevance from an applied and technological point of view is still largely appreciated. The Avrami model [eq. (6)] was used to obtain the n and Z parameters (Table II). These parameters, obtained for each sample at different crystallization temperatures (T_c), were then used to calculate the half-crystallization time $t_{1/2}$,[34] i.e. the time required to crystallize 50 mass % of the maximum amount of crystallizable material, as following

$$t_{1/2} = \left(\ln 2/Z\right)^{1/n} \tag{11}$$

The value of $t_{1/2}$ is particularly important for polymer processing. Table IV resumes the values of $t_{1/2}$. As previously pointed out (see the comments about Figure 7), the main consequence of the addition of a nucleating agent to PHB was a dramatic shift of the temperature range in which the polymer crystallization could be observed. This means that, while cooling down the polymer from the melt, the crystallization starts earlier but does not necessarily progress faster. In such a situation, the $t_{1/2}$ values cannot be used for a direct comparison of neat and

Table IV. Half-Crystallization Time (min) for Neat and Nucleated PHB at Different T_c

Sample/T_c (°C)	100	105	110	115	120	125
PHB	1.2	2.6	3.6	5.7	14.5	25.9
Sample/T_c (°C)	125	130	135	140	145	150
+BN NX1 0.2 %	0.8	1.8	4.6	10.4	21.2	-
+BN NX1 0.4 %	-	1.4	3.2	7.0	14.0	27.9
+BN NX1 0.8 %	-	1.0	2.3	5.4	9.5	20.6

nucleated PHBs. Indeed, the distribution of $t_{1/2}$ values over the crystallization temperature range for both neat and nucleated PHBs appeared to have more or less the same width (1.2 min $< t_{1/2} <$ 25.9 min for neat PHB vs. 0.8 min $< t_{1/2} <$ 27.9 min on average for nucleated PHBs). Nonetheless, Table IV presents also the half-crystallization time values at a crystallization temperature which is common to all the samples ($T_c = 125°C$). At $T_c = 125°C$, neat PHB is half-crystallized in about 26 min whereas the addition of only 0.2 wt % of BN NX1 reduces the half-crystallization time to 48 s.

CONCLUSIONS

The crystallization of neat PHB requires high supercooling degrees and progresses following the crystal growth Regime III. The crystal growth front is expected to be rough and irregular because of an intensive and multiple nucleation process. A fraction of tie macromolecules and/or polymer chains forming loops hinders a regular crystallization. As previously reported in the literature, it was found that the addition of boron nitride reduces the size of the nuclei required for crystal growth, which in turns allows the polymer to crystallize from the melt at lower supercooling degrees. WAXD spectra confirmed that the presence of the nucleating particles has no discernable effect on the crystalline arrangement of PHB macromolecules but, as expected, it drastically reduced the size of the spherulites. In spite of the technical issues encountered with optical microscopy observations for nucleated PHBs, the radial growth G could be estimated by processing DSC data through a rearranged Hoffman-Lauritzen equation. This work proved, for neat PHB, that such a method can be used to obtain the main parameters describing the crystallization phenomena, such as K_g or σ_e, whenever the optical microscopy techniques reach their limits. As a consequence of a crystallization which could take place at higher temperatures, a transition from Regime III to Regime II could be detected for nucleated PHBs. The addition of a nucleating agent made the crystal growth front more regular and therefore reduced the coupling between the crystalline and the amorphous phases. These modifications of the crystallization mechanisms were found to coherently explain the decrease of the fold surface free energy and of the glass transition temperature upon addition of the nucleating agent. A higher mobility of the polymer chains in the amorphous phase could be deduced for nucleated PHBs. The hypothesis of a less disordered (or more perfect) crystallization obtained upon addition of the nucleating agent is corroborated by the modifications of the endothermic peak which was observed during the heat scan of the thermal analysis performed on nucleated PHBs. In fact, the thermal analysis of neat PHB formerly revealed a bimodal melting behavior, due to the melting of the initially formed crystalline phase followed by a recrystallization and finally a second melting. For nucleated PHB, only a melting occurs due to a more perfect crystallization. It was also found that the crystallinity degree was not influenced by the presence of the nucleated agent. Finally, no dramatic differences were observed in the crystallization mechanisms and crystal growth rate for nucleated PHBs as a consequence of a change in the concentration of the nucleating agent; in particular, a concentration of 0.2 wt % was found to be sufficient to modify PHB crystallization behavior.

REFERENCES

1. Pan, P.; Inoue, Y. *Prog. Polym. Sci.* **2009,** *34*, 605.
2. Ye, H. M.; Wang, Z.; Wang, H. H.; Chen, G. Q.; Xu, J. *Polymer* **2010,** *51*, 6037.
3. Courgneau, C., Domenek, S., Guinault, A., Averous, L., Ducruet, V. *J. Polym. Environ.* **2011,** *19*, 362.
4. Somleva, M. N.; Snell, K. D.; Beaulieu, J.; Peoples, O. P.; Garrison, B.; Patterson, N. (Metabolix, Inc.) US 271,889, October 29, **2009.**
5. Wang, L.; Wang, X.; Zhu, W.; Chen, Z.; Pan, J.; Xu, K. *J. Appl. Polym. Sci.* **2009,** *116*, 1116.
6. Qian, J.; Zhu, L.; Zhang, J.; Whitehouse, R. *J. Polym. Sci.* **2007,** *45*, 1564.
7. Xing, P.; Ai, X.; Dong, L.; Feng, Z. *Macromolecules* **1998,** *31*, 6898.
8. Barker, P. A.; Barham, P. J.; Martinez-Salazar, J. *Polymer* **1997,** *38*, 913.
9. Cai, H.; Qiu, Z. *Phys. Chem. Chem. Phys.* **2009,** *11*, 9569.
10. Liu, W. J.; Yang, H. L.; Wang, Z.; Dong, L. S.; Liu, J. J. *J. Appl. Polym. Sci.* **2002,** *86*, 2145.
11. Dong, T.; Mori, T.; Aomaya, T.; Inoue, Y. *Carbohydr. Polym.* **2010,** *80*, 387.
12. Suksut, K.; Deeprasertkul, C. *J. Polym. Environ.* **2011,** *19*, 288.
13. Dargent, E.; Denis, A.; Galland, C.; Grenet, J. *J. Thermal Anal.* **1996,** *46*, 377.
14. Hoffman, J. D.; Lauritzen, J. I. *J. Res. Natl. Bur. Stand.* **1961,** *65A*, 297.
15. Sobkowicz, M. J.; Dorgan, J. R.; Gneshin, K. W.; Herring, A. M.; McKinnon, J. T. *J. Polym. Environ.* **2008,** *16*, 131.
16. Grady, B. P.; Pompeo, F.; Shambaugh, R. L.; Resasco, D. E. *J. Phys. Chem. Part B* **2002,** *106*, 5852.
17. Naiki, M.; Fukui, Y.; Matsumura, T.; Nomura, T.; Matsuda, M. *J. Appl. Polym. Sci.* **2000,** *79*, 1693.
18. Assouline, E.; Lustiger, A.; Barber, A. H.; Cooper, C. A.; Klein, E.; Wachtel, E.; Wagner, H. D. *J. Polym. Sci. Part B; Polym. Phys.* **2002,** *41*, 520.
19. Zhang, L.; McCarthy, S.; Whitehouse, R. *J. Appl. Polym. Sci.* **2004,** *94*, 483.
20. Mandelkern, L. In Physical Properties of Polymers; Mark, J. E.; Eisenberg, A.; GraessleyW. W., Eds.; ACS; American Chemical Society: Washington, DC, **1999.**
21. Don, T. M.; Chen, P. C.; Shang, W. W.; Chiu, H. S. *Tamkang J. Sci. and Eng.* **2006,** *9*, 279.
22. Hoffman, J. D.; Frolen, L. J.; Ross, G. S.; Lauritzen, J. I. *J. Res. Natl. Bur. Stand. A* **1975,** *79*, 671.
23. Hoffman, J. D. *Polymer* **1983,** *24*, 3.
24. Ferry, J. D. Viscoelastic Properties of Polymers; Wiley: New York, **1970.**
25. Williams, M. L.; Landel, R. F.; Fery, J. D. *J. Am. Chem. Soc.* **1955,** *77*, 3701.
26. Peng, S.; An, Y.; Chen, C.; Fei, B.; Zhuang, Y.; Dong, L. *Eur. Polym. J.* **2003,** *39*, 1475.

27. Hoffman, J. D.; Weeks, J. J. *J. Res. Natl. Bur. Stand.* **1962,** *A66*, 13–28.
28. Yamada, K.; Hikosaka, M.; Toda, A.; Yamazaki, S.; Tagashira, K. *Macromolecules* **2003,** *36*, 4802.
29. Doudou, B. B.; Dargent, E.; Grenet, J. *J. Thermal Anal.* **2006,** *85*, 409.
30. Chen, G. X.; Hao, G. J.; Guo, T. Y.; Song, M. D.; Zhang, B. H. *J. Appl. Polym. Sci.* **2003,** *93*, 655.
31. Xing, P.; Dong, L.; An, Y.; Feng, Z.; Avella, M.; Masturcelli, E. *Macromolecules* **1997,** *30*, 2726.
32. Skrbic, Z.; Divjakovic, V. *Polymer* **1995,** *37*, 505.
33. Pan, P.; Liang, Z.; Nakamura, N.; Toshio, M.; Yoshio, I. *Macromol. Biosci.* **2009,** *9*, 585.
34. Kai, W.; He, Y.; Inoue, Y. *Polym. Int.* **2005,** *54*, 780.
35. Donth, E.; Korus, J.; Hempel, E.; Beiner, M. *Thermochim. Acta* **1997,** *304/305*, 239.
36. Delbreilh, L.; Dargent, E.; Grenet, J.; Saiter, J. M.; Bernes, A.; Lacabanne, C. *Eur. Polym. J.* **2007,** *43*, 249.
37. Arabeche, K.; Delbreilh, L.; Adhikari, R.; Michler, G. H.; Hiltner, A.; Baer, E.; Saiter, J. M. *Polymer* **2012,** *53*, 1355.
38. Delbreilh, L.; Bernes, A.; Lacabanne, C.; Grenet, J.; Saiter, J. M. *Mater. Lett.* **2005,** *59*, 2881.
39. Righetti, M. C.; Tombari, E.; Di Lorenzo, M. L. *Eur. Polym. J.* **2008,** *44*, 2659.
40. Bartolotta, A.; Di Marco, G.; Farsaci, F.; Lanza, M.; Pieruccini, M. *Polymer* **2003,** *44*, 5771.
41. Delpouve, N.; Saiter, A.; Dargent, E. *Eur. Polym. J.* **2011,** *47*, 2414.
42. Jeziorny, A. *Polymer* **1978,** *19*, 1142.
43. Liu, J. J.; Tang, G. B.; Qu, G. J.; Zhou, H. R.; Guo, Q. P. *J. Appl. Polym. Sci.* **1993,** *47*, 2111.
44. Maffezzoli, A.; Kenny, J. M.; Torre, L. *Thermochim. Acta* **1995,** *269/270*, 185.
45. Avrami, M. *J. Am. Chem. Phys.* **1939,** *7*, 1103.
46. Hoffman, J. D. *Polym. Papers* **1984,** *26*, 803.
47. Mitomo, H.; Barham, P. J.; Keller, A. *Polym. J.* **1987,** *19*, 1241.
48. Hoffman, J. D.; Lauritzen, J. I. *J. Res. Natl. Bur. Stand. A* **1961,** *65*, 297.
49. Lauritzen, J.; Hoffman, J. D. *J. Appl. Sci.* **1973,** *44*, 4340.
50. Hoffman, J. D.; Miller, R. L.; Marand, H.; Roitman, D. B. *Macromolecules* **1992,** *25*, 2221.
51. Hoffman, J. D. *Polymer* **1985,** *26*, 803.
52. Keith, H. D.; Padden, F. L. *J. Appl. Phys.* **1964,** *35*, 1270.
53. Clark, E. J.; Hoffman, J. D. *Macromolecules* **1984,** *17*, 878.